

**ANALYSIS OF ALLENDE NANODIAMOND RESIDUE BY CORRELATED TRANSMISSION ELECTRON MICROSCOPY AND ATOM-PROBE TOMOGRAPHY.** J. B. Lewis<sup>1,2</sup>, D. Isheim<sup>4</sup>, C. Floss<sup>1,2</sup>, T. L. Daulton<sup>2,3</sup>, D. N. Seidman<sup>4</sup>, <sup>1</sup>Laboratory for Space Sciences, <sup>2</sup>Physics Dept., Washington University, <sup>3</sup>Institute of Materials Science and Engineering, St. Louis, MO, <sup>4</sup>Center for Atom-Probe Tomography, Dept. of Materials Science and Engineering, Northwestern University, Evanston, IL. Email: jblewis@go.wustl.edu

**Introduction:** The study of isotopic anomalies in potentially presolar, meteoritic nanodiamonds (NDs) by atom-probe tomography (APT) [1–3] has been hampered by uncertainties in ND size and location, as well as the presence of non-diamond material in the ND separates [4–6]. The correlated acquisition of data from transmission electron microscopy (TEM) and APT is a powerful approach for the characterization of nanostructures and nanoparticles [7–12]. Therefore, we have performed correlated TEM/APT investigations of three samples from the Allende DM ND separate.

**Methods:** The Allende DM separate was created by crushing Allende fragments and subjecting them to acid dissolution to isolate refractory grains carrying Xe-HL gases [4]. A droplet of deionized water containing this “acid residue” was placed on a Pt surface and the liquid allowed to evaporate, leaving behind a ring of solids. This deposition layer was covered with another layer of sputter-deposited Pt. Focused Ion Beam (FIB) milling was used to lift out portions of the deposition, attach them to the end of electropolished and FIB-tapered Cu half-grid microposts, and sharpen them to a ~25 nm radius, with the plane of the ND deposition layer lying along the axis of the microtip (Fig. 1a).

TEM analysis was conducted using a JEOL 2100F scanning TEM at Washington University in St. Louis. During TEM analysis, residual hydrocarbons on the specimen grid and in the vacuum deposited on the microtips in several cases (see Fig. 1b). Images were taken at various angles around the microtip shaft, ranging from perpendicular to the deposition layer to 35 degrees off-perpendicular.

After TEM analysis, a ~50 nm layer of Ni was sputter-deposited on the microtips to increase the stability of the multilayer during APT analysis.

APT was then conducted using the LEAP 4000X Si at Northwestern University. The microtips were field-evaporated atom-by-atom at ~10 kV DC voltage with thermal activation from a pulsed 355 nm laser. Time-of-flight mass spectrometry, point-projection microscopy, and ion detection sequence were used to reconstruct the mass-to-charge-state ratios and original 3D positions of up to 50% of the atoms in the volume analyzed, with sub-nm spatial resolution and mass resolution sufficient to distinguish <sup>12</sup>C and <sup>13</sup>C.

**Results:** Using conventional bright-field and scanning HAADF imaging, we detected low-density features in the deposition layers of three microtips, HG01-A, -B, and -C (Fig. 1b–d). These features are similar in size to each other, are on the order of 1–10 nm in diameter, and are composed of significantly lower-Z material than Pt, consistent with NDs. Furthermore, TEM tilt series images were used to view stereopairs of the tips in three-dimensions and the discrete features observed appeared coplanar in the orientation of the ND deposition layer. Only microtips with a thick ND-deposit in the tip, as imaged by secondary electrons in the SEM, contained the discrete features observed by TEM.

APT was conducted on tips HG01-B and -C. Reconstructions (Fig. 1e) show a deposition layer within each tip distinguishable by higher C concentration than in the surrounding Pt. The deposition layers also contain Na, NaO, Cl, and F, known contaminants resulting from the acid treatments carried out to isolate the NDs from the Allende host. These residue constituents are not observed in all atom-probe studies of NDs; rather, they are associated only with liftouts from the inner edge of a relatively thick ND deposit. Microtips created from the outer edges of ND deposits contain only insignificant concentrations of these contaminants. The deposition layers also contain implanted Ga from FIB sharpening, as well as Ni from sputter deposition. The concentrations of these contaminants fall off with depth into the deposition layer, whereas the C concentrations do not, further distinguishing the deposition layers from the hydrocarbon caps accidentally deposited by the TEM beam. In contrast to the TEM data, the C was strewn throughout the deposition layers at too low a density to represent NDs, and no ND-sized regions of higher C-density were detected in the APT reconstructions, nor were any voids.

**Discussion:** We posit two possible explanations for why TEM analyses show a number of isolated, low-density regions of a few nm in size embedded in a plane in the Pt, while APT data shows a C-strewn deposition plane with no isolated or higher-density clusters of C:

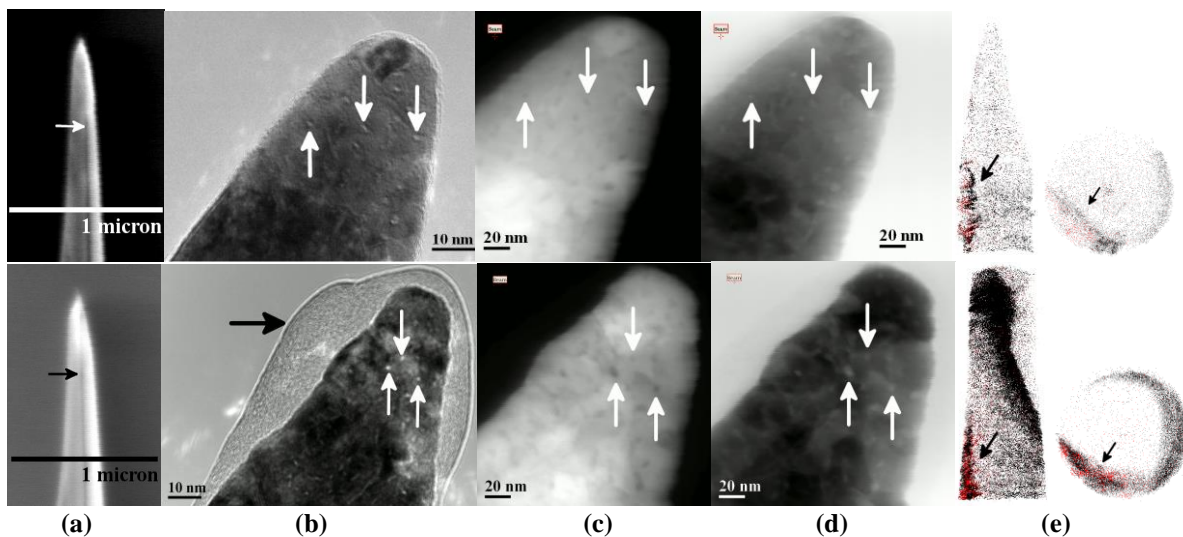


**Figure 1:** Secondary electron images of microtips HG01-B (top) and HG01-C (bottom) taken after sharpening and prior to TEM analysis (a) show the deposition layer (arrow) between Pt layers. TEM bright-field images (b) as well as high angle annular dark field (c) and bright field (d) images show low-density features, as well as a hydrocarbon cap on HG01-C. Atom-probe reconstructions (e) of C (black) and NaO (red) ions show C-strewn deposition layers. HG01-C has a hydrocarbon cap, distinguished from the Allende residue in this image by its orientation and the absence of NaO.

1) The low-density regions observed by TEM are not actually NDs; rather, they are voids created when Pt was deposited onto a low-density, porous deposit consisting primarily of amorphous sp<sup>2</sup> carbon from the acid residue. Trajectory aberrations prevent these voids from being visualized in APT reconstructions.

2) The TEM images do reveal NDs, but these were plucked from a low-density deposit by the high electric field present during APT analysis before individual atoms could be field evaporated and detected. This is because the evaporation field required for diamond is considerably higher than that measured for Pt; indeed, past APT experiments have shown voids that may represent NDs plucked from the microtip while mostly intact.

**Outlook:** Since NDs have been detected in past work without the presence of a C-strewn deposition layer, Na, NaO, Cl, or F [1–3], it is clear that the amount of non-ND material contained in deposits of Allende DM separate varies significantly. Factors influencing the concentrations of various material include the concentration of material in the deposited droplet, the location of the liftout from the deposited ring, and other random factors.

Care should be taken to select FIB liftout locations under conditions that have yielded isolated NDs in past APT reconstructions, such as the outer-rims of thin deposits with slowly tapering deposit density.

Correlated TEM imaging of microtips prior to APT is shown to be a valuable technique, in this case revealing that either NDs or voids were being overlooked by APT reconstructions. By imaging microtips that contain isolated, high-density C clusters in APT reconstructions, we can assess whether the low-density TEM features are NDs or voids.

**References:** [1] Heck P. R. et al. (2014) *Meteorit. Planet. Sci.* 49 (3) 453–467. [2] Isheim D. et al. (2013) *Microsc. Microanal.* 19 (Suppl 2), CD974–CD975. [3] Lewis J. B. et al. (2015) *Ultramicroscopy* 159, 248–254. [4] Lewis R. S. et al. (1987) *Nature* 326, 160–162. [5] Stroud R. M. et al. (2011) *ApJL* 738, L27–L31. [6] Daulton T. L. et al. (2016) *J. Quatern. Sci., submitted*. [7] Baik S.-I. et al. (2013) *Scripta Mater* 68(11), 909–912. [8] Gorman B. P. et al. (2008) *Micro. Today* 16, 4, 42–47. [9] Henry K. T. (2012) *Micro. & Microanal.* 18, S2, 988–989. [10] Devaraj A. et al. (2014) *J. Phys. Chem. Lett.* 5, 1361–1367. [11] Herbig M. et al. (2015) *Ultramicroscopy* 153, 32–39. [12] Rout et al. (2015) *LPS XLVI*, Abstract #2938.

This work is supported by NASA grants NNX14AP15H (J.B.L.) and NNX13AF53G (C.F.), NSF-MRI DMR-0420532 and ONR-DURIP N00014-0400798, N00014-0610539, and N00014-0910781 (LEAP tomograph at NUCAPT), the Initiative for Sustainability and Energy at Northwestern University (Instrumentation at NUCAPT), and MRSEC NSF DMR-1121262 (NUCAPT, through Northwestern’s Materials Research Center).